

Measurements of the Higgs boson inclusive and differential fiducial cross-sections in the diphoton decay channel with pp collisions at $\sqrt{s} = 13$ TeV with the ATLAS detector

Muon Spectrometer

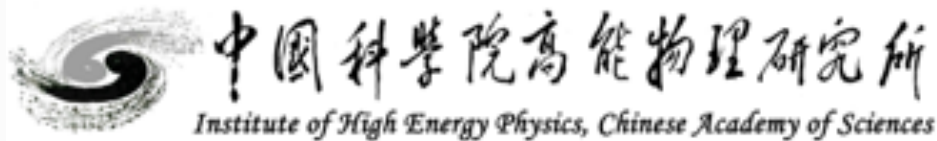
Inner Detector

Magnet System

Gangcheng Lu¹, on behalf of the ATLAS collaboration

¹IHEP, CAS

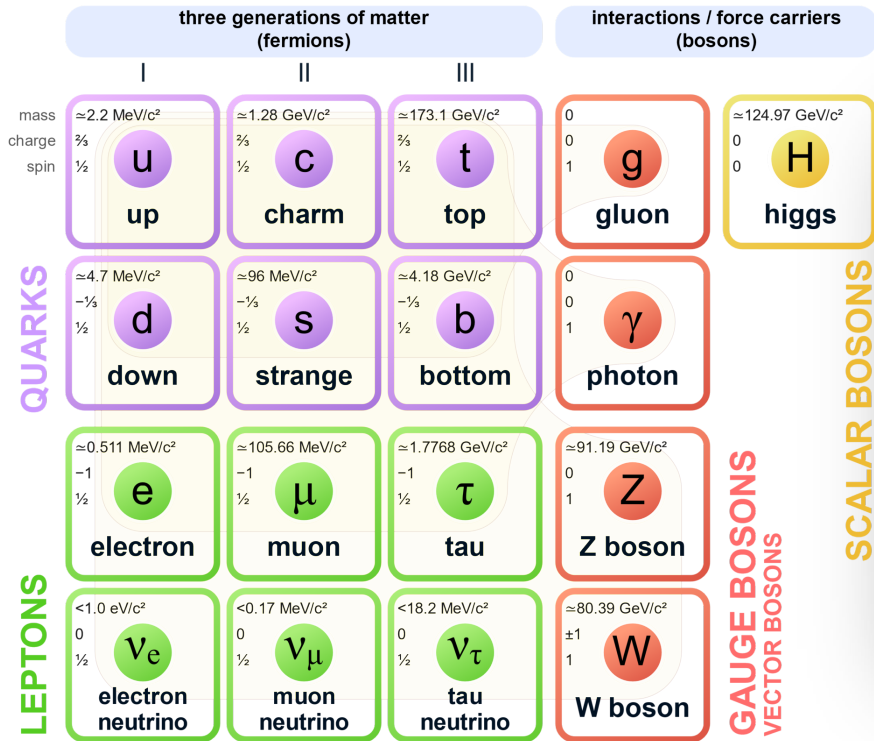
Higgs Potential 2022, July 25th



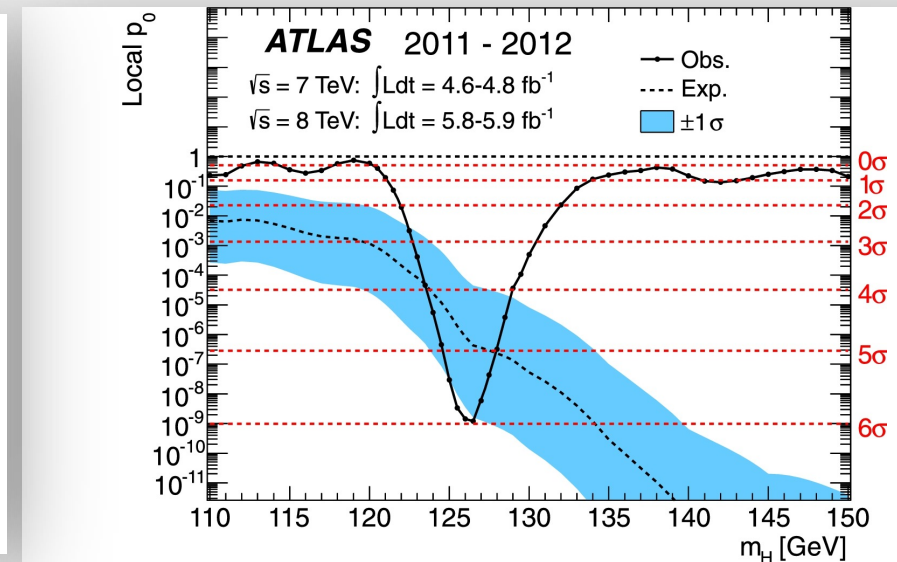
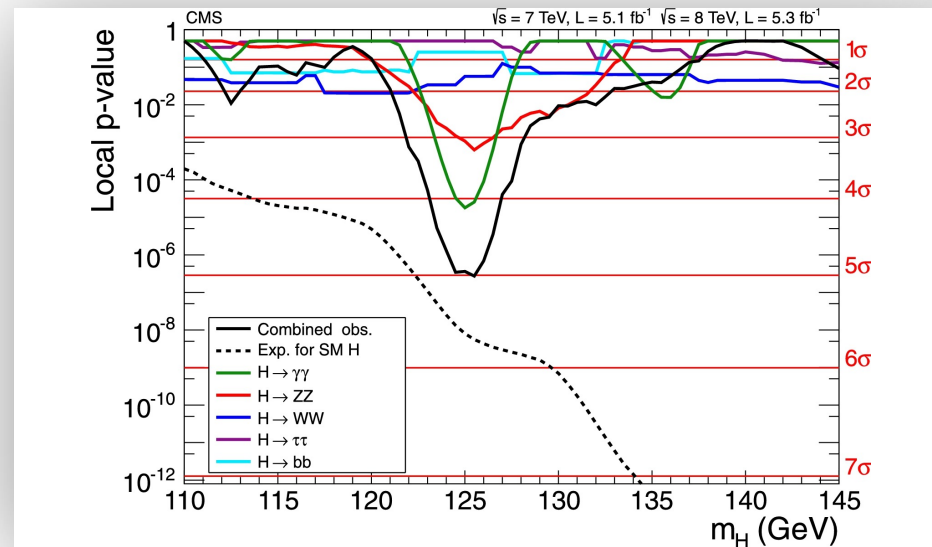
Standard Model and Higgs boson

- ◆ Standard Model describes fundamental particles and forces that make up our Universe
- ◆ Higgs boson is responsible for the masses of elementary particles, discovered by ATLAS and CMS 10 years ago, filling the last puzzle piece of SM

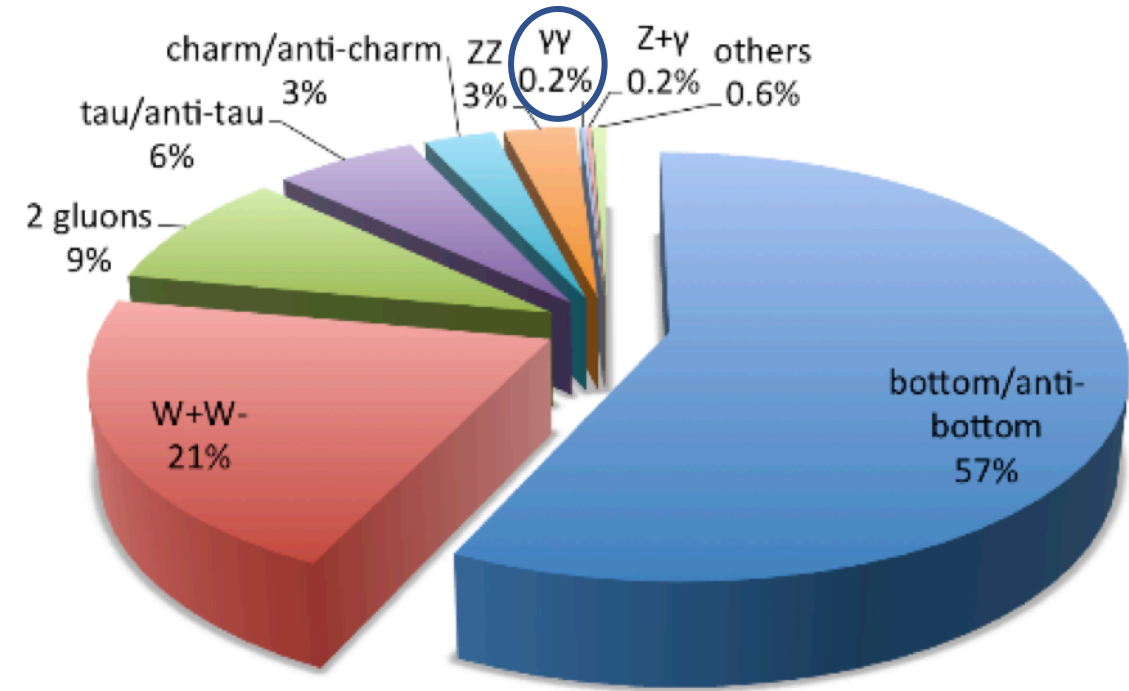
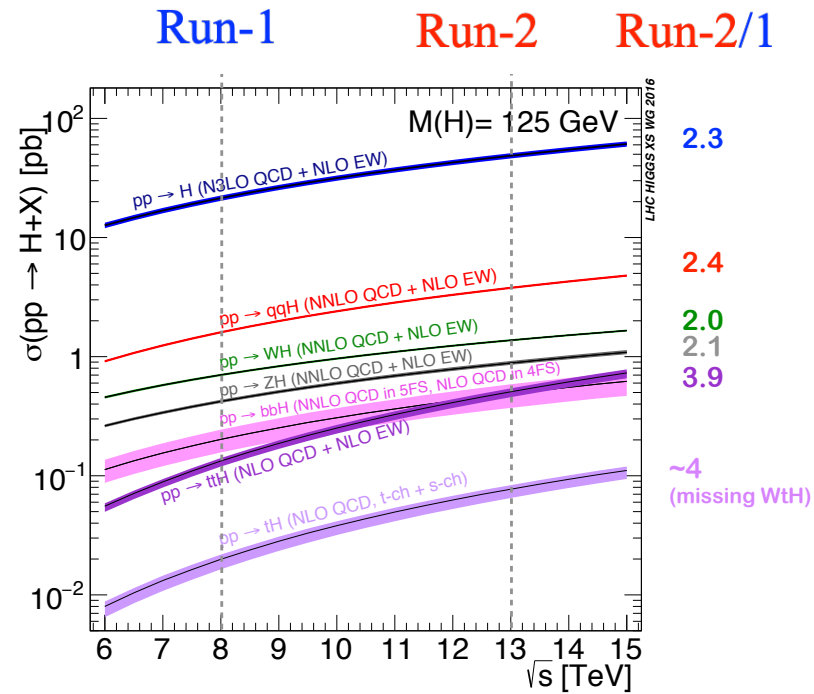
Standard Model of Elementary Particles



Discovery of Higgs boson opens a new era of particle physics

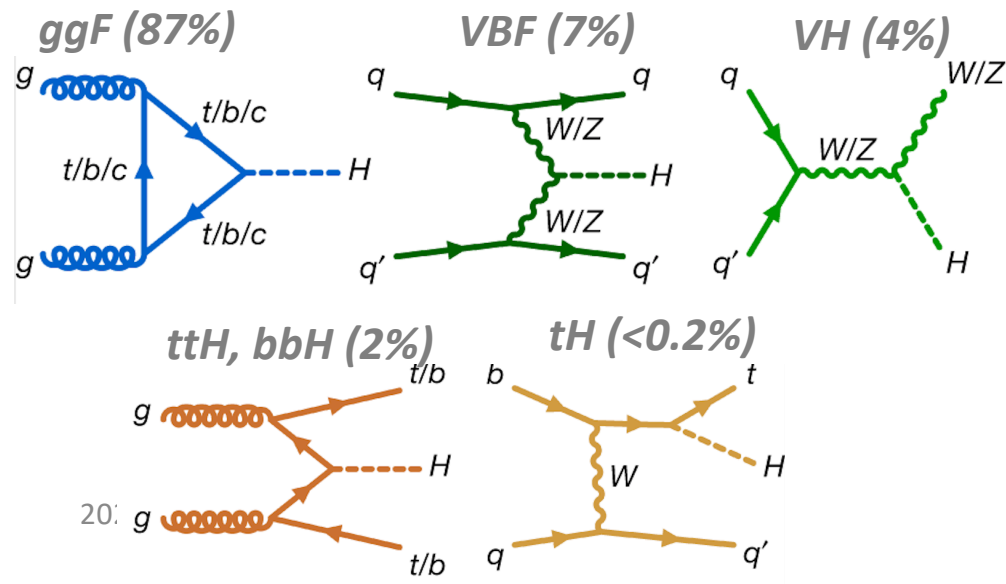


Production and decays of Higgs boson



Why $H \rightarrow \gamma\gamma$ important?

- ◆ Excellent photon reconstruction and identification efficiency lead to a high Higgs signal yield
- ◆ Nice signal-background separation
- ◆ Good photon resolution exhibits the Higgs signal a peak on top of a smoothly-falling background



How we measure Higgs properties in Run2

Run 1-style coupling measurements:
 μ , κ

Simplified template cross sections

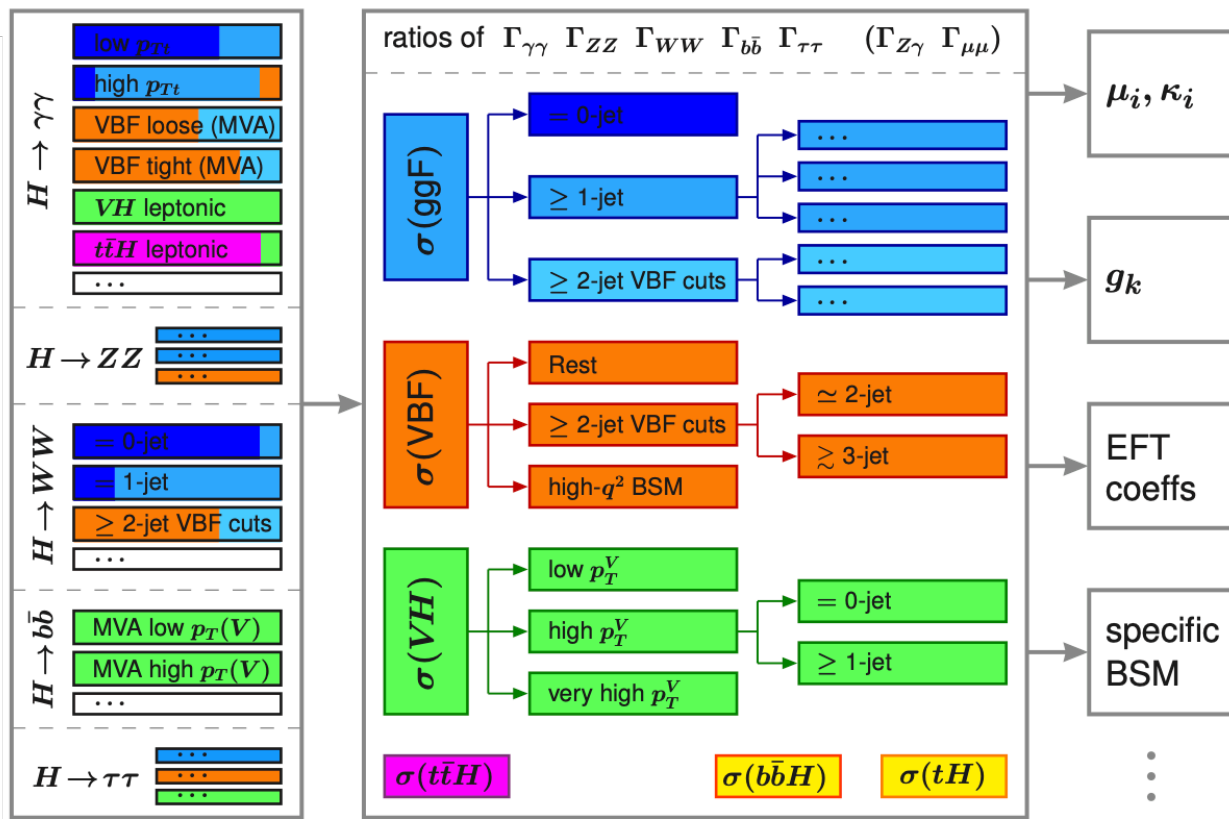
Fiducial/differential cross sections

Most model-independent measurement!

General workspace of fiducial XS measurements

Model independence

Analysis power

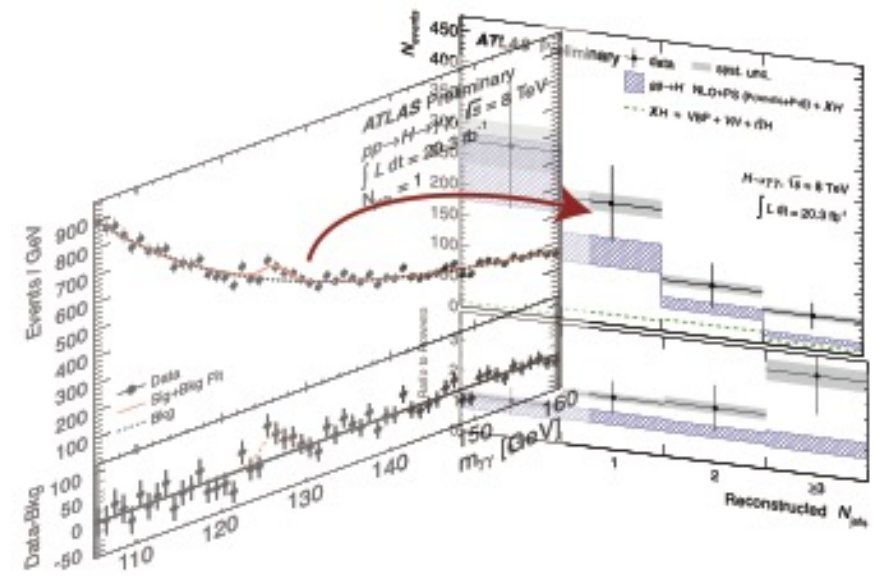


Reco-level yield
Fiducial

Unfolding

correct for
detector effects

Particle-level XS
Fiducial



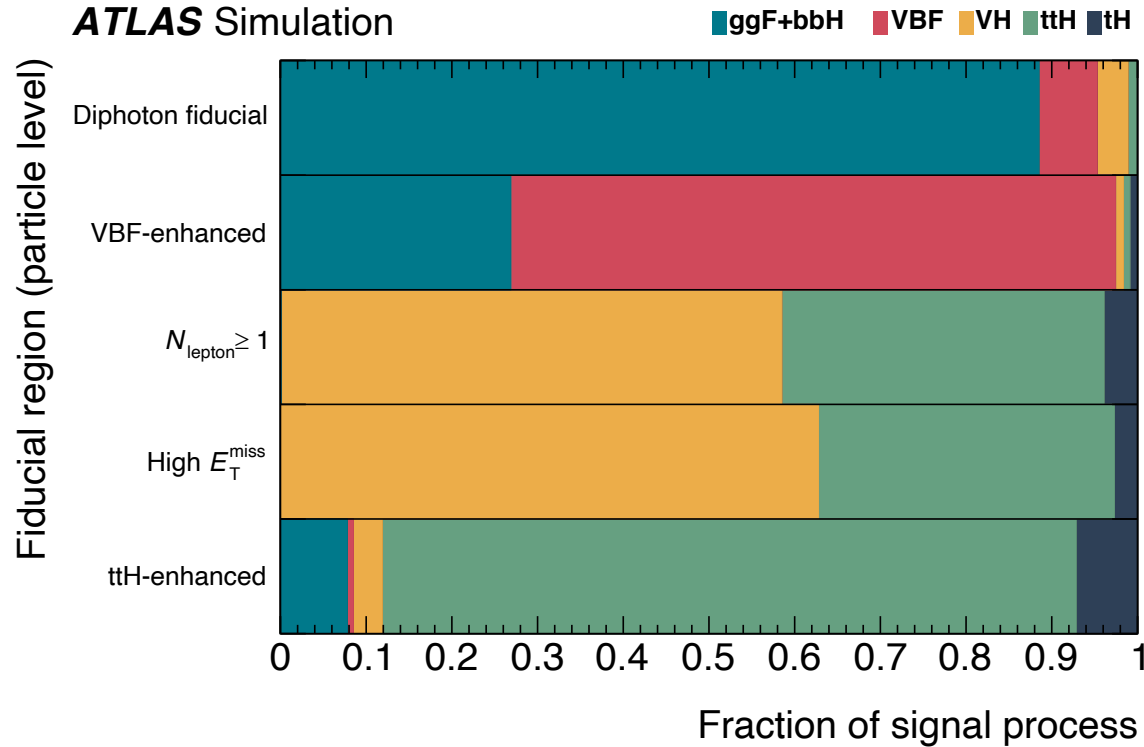
NP Corr.

Parton-level
Fiducial

Fid. Corr.

Parton-level
Inclusive

Definitions of $H \rightarrow \gamma\gamma$ fiducial phase space



Subsets of the diphoton baseline fiducial region are defined to provide phase-space regions sensitive to particular Higgs production modes

- ◆ **VBF-enhanced (VBF)**: at least 2 jets, $m_{jj} > 600$ GeV, $|\Delta y_{jj}| > 3.5$
- ◆ $N_{lepton} \geq 1$ (**VH**, **$t\bar{t}H$** and **tH**): at least one $e(\mu)$ with $p_T > 15$ GeV and $|\eta| < 2.47(2.7)$
- ◆ **High E_T^{miss} (VH, $t\bar{t}H$ and BSM effects)**: $E_T^{miss} > 80$ GeV and $p_T^{\gamma\gamma} > 80$ GeV
- ◆ **$t\bar{t}H$ -enhanced ($t\bar{t}H$ and tH)**: ≥ 1 b-jet AND (≥ 1 lepton, ≥ 3 jets) OR (0 leptons, ≥ 4 jets))

Baseline Diphoton fiducial volume (to mimic detector-level acceptance region):

At least 2 isolated prompt photons, $|\eta| < 1.37$ or $1.52 < |\eta| < 2.37$, $p_T/m_{\gamma\gamma} > 0.35$ and 0.25

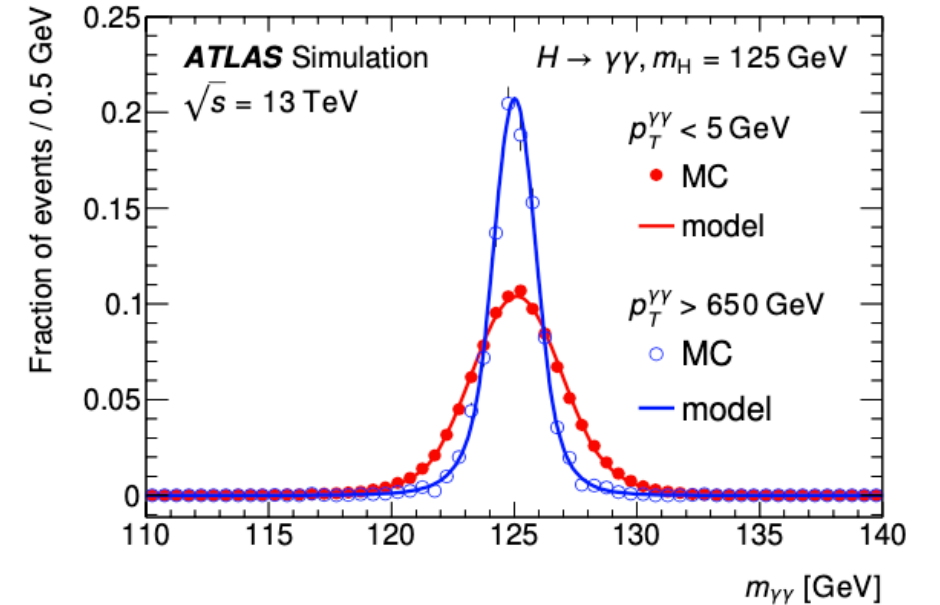
Signal and background modeling

Signal modeling

- ◆ **Double-sided Crystal Ball** function used. Individual fit to $m_{\gamma\gamma}$ distribution in each analysis bin independently.

Background modeling

- ◆ Main source of background is non-resonant $\gamma\gamma$ and γj . Fractions of background components measured using a **2x2D side-band method**.
- ◆ A spurious signal test used to determine bkg. function, which requires $S/S_{ref} < 10\%$ and $S/\Delta S < 20\%$. **GPR approach** exploited to smoothen background template to suppress statistical fluctuations, that can reduce SS by 30% in average



	$\gamma+jet$			$jet+jet$
	AD	CD	BD	DD
subleading γ not isolated	TL'	L'L'	TL'	L'L'
	AB	CB	BB	DB
	TT	L'T	TT	L'T
subleading γ isolated	AC	CC	BC	DC
	TL'	L'L'	TL'	L'L'
	$\gamma\gamma$	CA	BA	$jet+\gamma$
	AA	CA	BA	DA
	TT	L'T	TT	L'T
	leading γ isolated		leading γ not isolated	

AA is SR. AD and DA corresponds to γj CR

Systematic uncertainties

Affect signal or background shape

- ◆ **Photon energy scale uncertainty:** shift signal peak position
- ◆ **Photon energy resolution uncertainty:** broaden or narrow signal width
- ◆ **Spurious signal uncertainty:** originated from choice of background model

Others

- ◆ **Luminosity uncertainty:** 1.7%
- ◆ **BR of Dalitz decays:** usually < 1%

Affect response matrix

◆ Experimental

- ◆ Diphoton trigger efficiency, Vertex selection efficiency, Photon ID/ISO efficiency, Photon energy scale/resolution, pile-up, JET, Lepton, E_T^{miss} , b-tagging

◆ Theoretical

- ◆ **Signal composition:** estimated by varying XS of each production mode within its measured uncertainty
- ◆ **Modeling of matrix element generator:** estimated by difference between response matrix from nominal Powheg and alternative MadGraph5
- ◆ **Modeling of parton shower, underlying event and hadronization:** estimated from switching PS algorithm from nominal Pythia8 to Herwig7

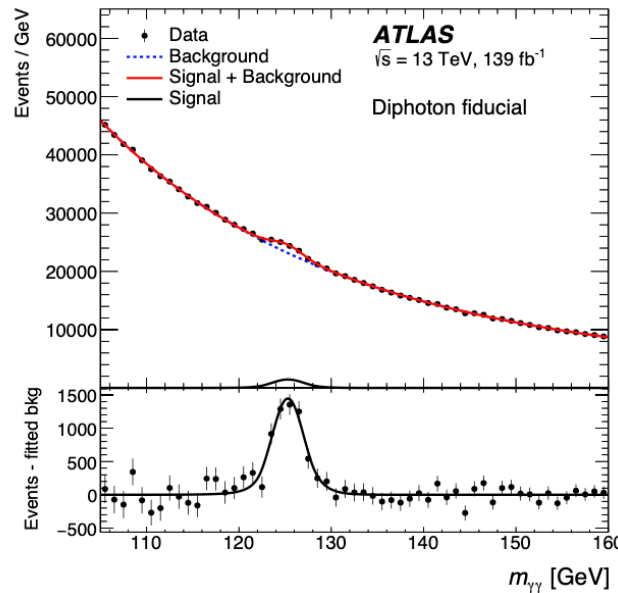
Unfolding (from N_{reco} to particle-level cross-sections)

A simultaneous fit of all the reco-bins for a given observable

Measured cross-sections, compared with various predictions directly

Determine sig. parameters and bkg. function

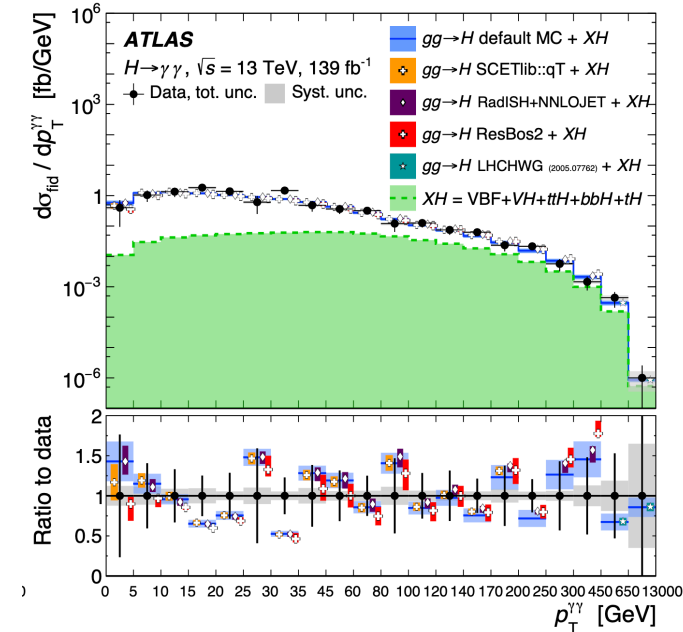
Modeling of signal and background



N_r parameterized as function of XS via Response Matrix R



$$N_r^{(H)} = \frac{1}{C_r^{fid}} \left[\sum_t L \times (\sigma_t \times B_{\gamma\gamma}) \times R_{t,r} \right],$$



C_r^{fid} corrects for events that pass selection but outside of the fiducial region.

$R_{t,r}$ is the probability for a signal event generated in truth-bin t to be selected in reco-bin r . They are estimated from SM simulations taking into account all the production modes

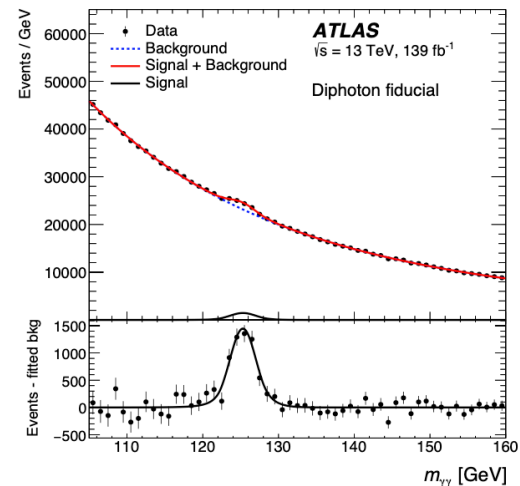
H $\rightarrow\gamma\gamma$ $\sqrt{s}=13$ TeV ATLAS Simulation

$N_{jets} (true)$		≥ 3	$=2$	$=1$	$=0$
$N_{jets} (reco)$	≥ 3	1	9	60	
	$=2$	1	8	50	10
	$=1$	8	51	11	2
	$=0$	59	8	1	
		≥ 3	$=2$	$=1$	$=0$

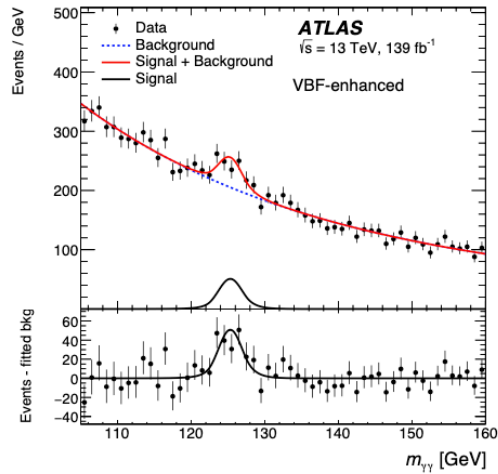
Response matrix of N_{jets}

Fiducial cross-section measurements

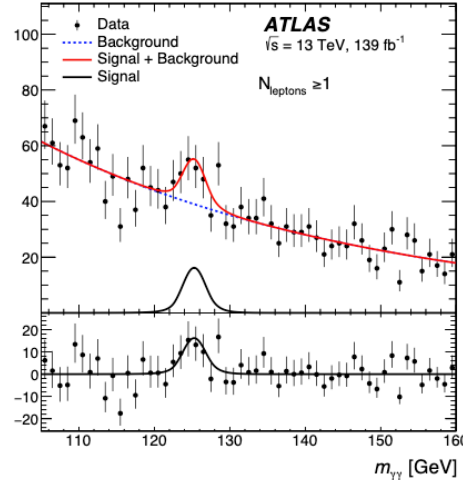
Diphoton baseline



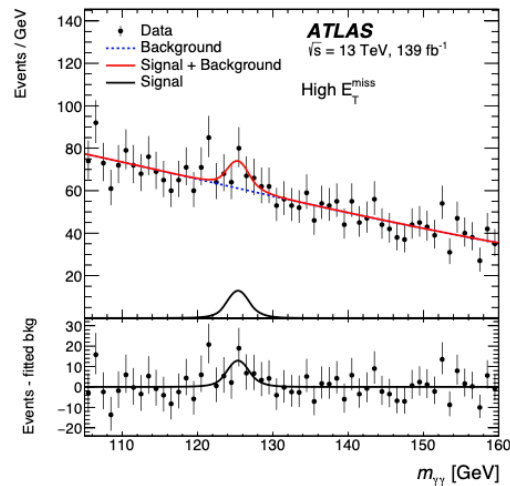
VBF-enhanced



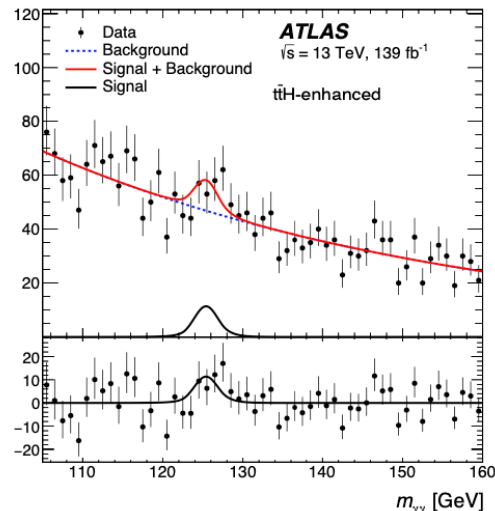
$N_{lep} \geq 1$



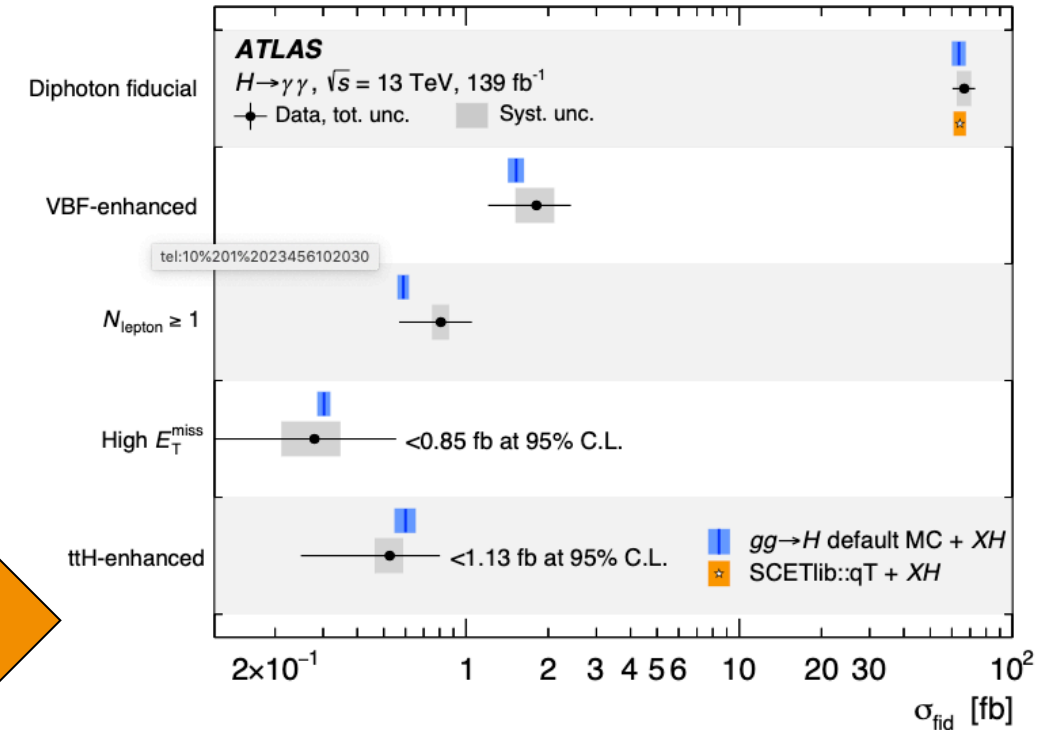
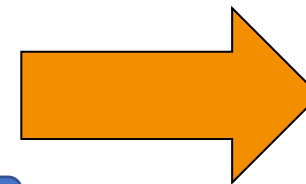
High E_T^{miss}



ttH-enhanced



Unfolding



Diphoton fiducial XS times $BR_{\gamma\gamma}$ measured to

be:

$\sigma_{fid} = 67 \pm 5(stat.) \pm 4(sys.) fb$, compatible with SM predicted $\sigma_{fid}^{SM} = 64 \pm 4 fb$

Extrapolated to total Higgs production phase space:

$\sigma_{tot} = 58 \pm 4(stat.) \pm 4(sys.) pb$

Binning definitions of differential variables

~30 differential variables included in the paper:

Diphoton
fiducial

Diphoton kinematic	$p_T^{\gamma\gamma}, y_{\gamma\gamma} , p_T^{\gamma 1}/m_{\gamma\gamma}, p_T^{\gamma 2}/m_{\gamma\gamma}$
Jet multiplicities	$N_{\text{jets}}, N_{\text{b-jets}}$
1-jet inclusive	$p_T^{j1}, H_T, p_T^{\gamma\gamma j}, m_{\gamma\gamma j}, \tau_{C,j1}, \Sigma\tau_{C,j}$
2-jet inclusive	$m_{jj}, \Delta\phi_{jj}, \Delta\phi_{\gamma\gamma,jj} , p_T^{\gamma\gamma jj}$
2D differential	$p_T^{\gamma\gamma}$ vs $ y_{\gamma\gamma} , p_T^{\gamma\gamma}$ vs $p_T^{\gamma\gamma j}, p_T^{\gamma\gamma}$ vs $\tau_{C,j1}, (p_T^{\gamma 1} + p_T^{\gamma 2})/m_{\gamma\gamma}$ vs $(p_T^{\gamma 1} - p_T^{\gamma 2})/m_{\gamma\gamma}$
Jet-veto	$p_T^{\gamma\gamma}$ jetveto 30GeV, $p_T^{\gamma\gamma}$ jetveto 40GeV, $p_T^{\gamma\gamma}$ jetveto 50GeV, $p_T^{\gamma\gamma}$ jetveto 60GeV
VBF-enhanced	VBF $ \eta^* , \text{VBF } \Delta\phi_{jj}, \text{VBF } p_T^{j1}, \text{VBF } p_{T,\gamma\gamma jj}, \text{VBF } p_T^{j1}$ vs $\Delta\phi_{jj}$

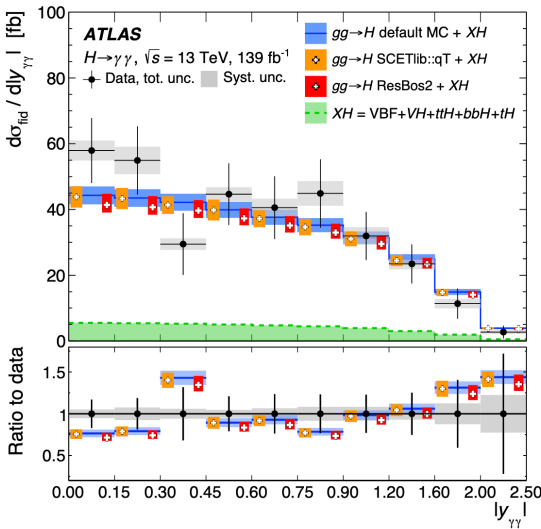
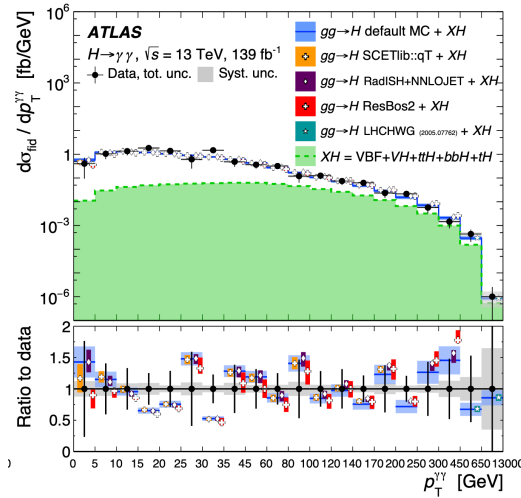
Probe very wide regions of phase space

The binning determined using following principles:

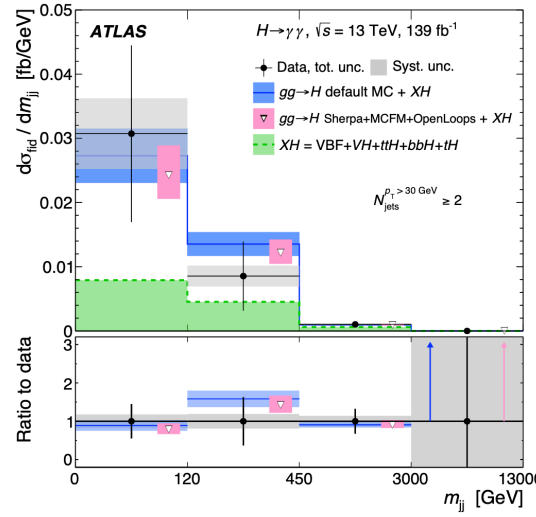
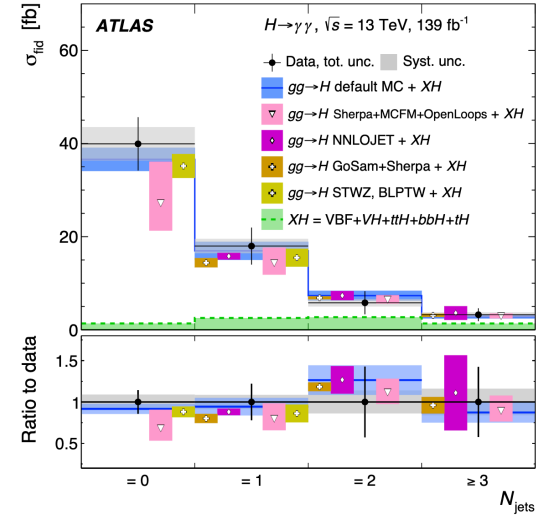
- ◆ An expected signal significance close to or greater than 2σ
- ◆ A migration purity close to or higher than 50%
- ◆ Unification with HZZ analysis as possible (eventually CMS), for future combination

Differential fiducial cross-section measurements

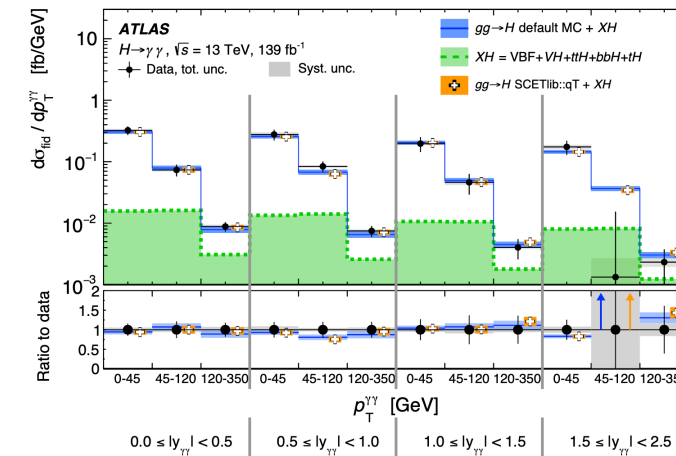
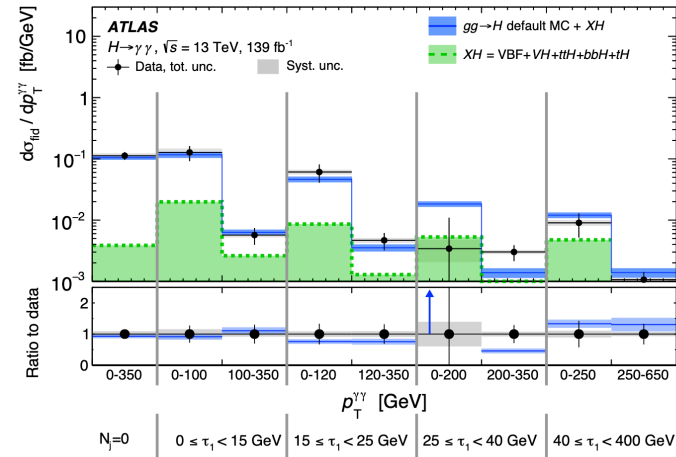
Kinematic



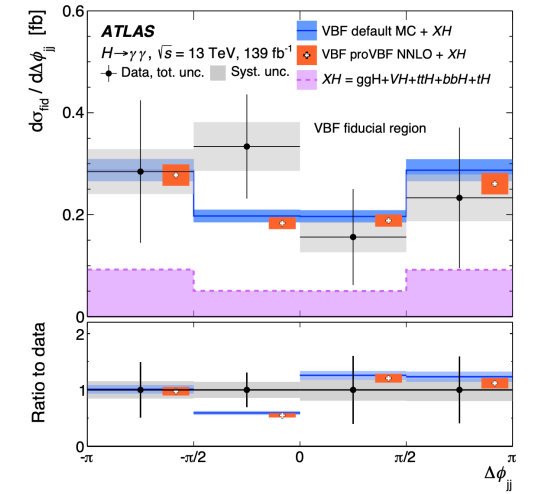
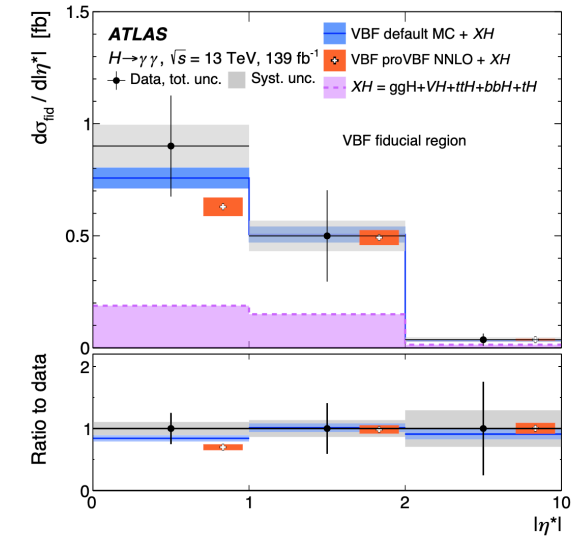
Jet-related



2D differential



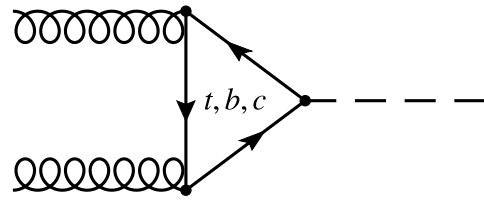
VBF-enhanced



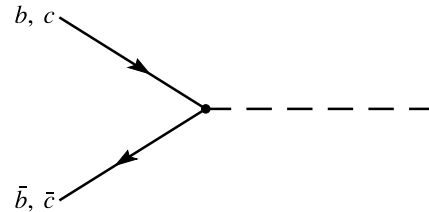
The measurements compatible with various predictions at different orders of QCD accuracy (such as **MATRIX+RaDISH**, **ResBos2**, **SCETlib::qT**)

Limits on the b - and c -quark Yukawa coupling

2 primary productions in the study



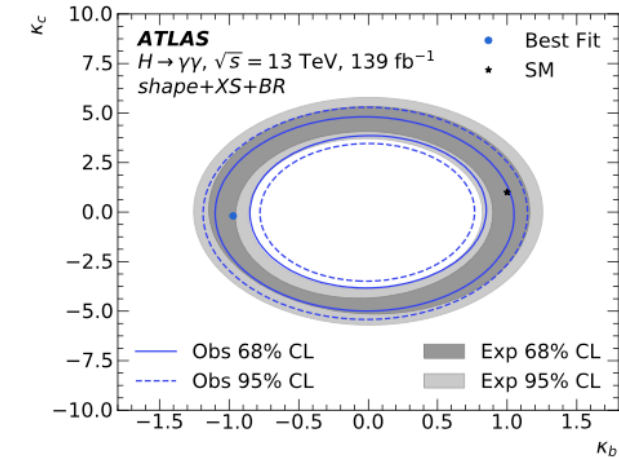
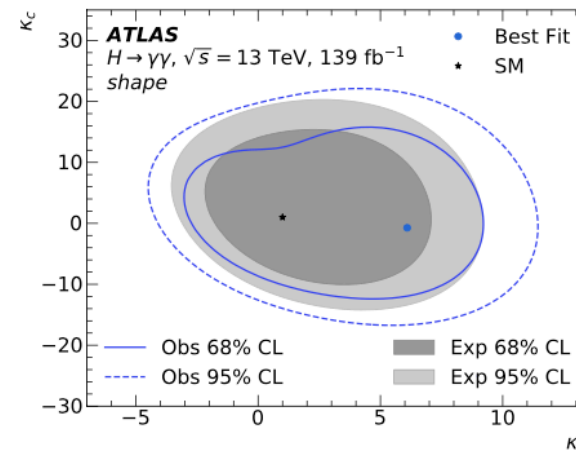
Gluon-gluon fusion



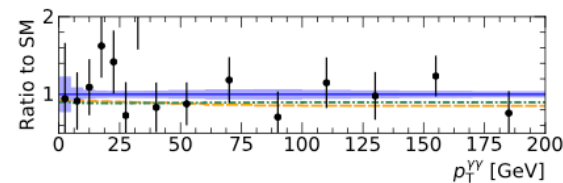
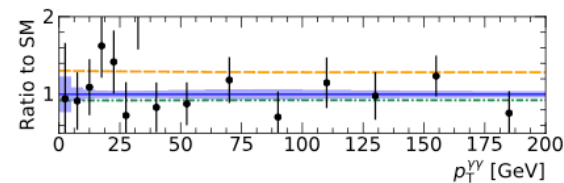
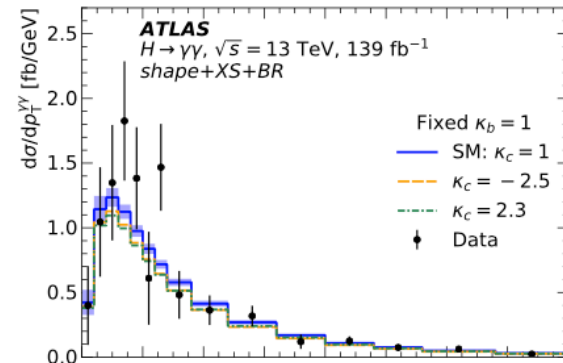
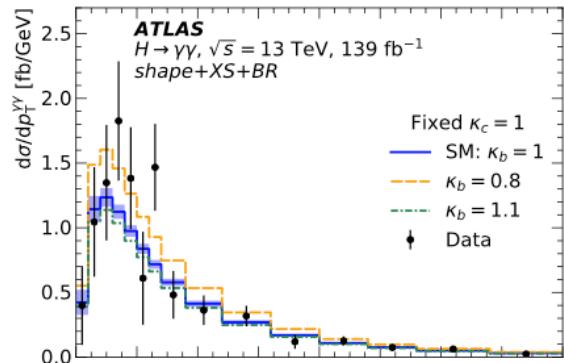
Quark-initiated

Two fitting strategy studied:

- ◆ Only consider variation of shape (**shape**)
- ◆ Consider also the normalization of cross-section times branching ratio (**shape+XS+BR**)



Probe κ_b and κ_c indirectly through the measured $p_T^{\gamma\gamma}$ spectrum



Fit set-up	κ	Observed 95% CL	Expected 95% CL
Shape-only	κ_c	$[-12.6, 18.3]$	$[-10.1, 17.3]$
	κ_b	$[-3.5, 10.3]$	$[-2.5, 8.1]$
Shape+normalisation (with branching ratio variations)	κ_c	$[-2.5, 2.3]$	$[-3.0, 3.1]$
	κ_b	$[-1.1, -0.8] \cup [0.8, 1.1]$	$[-1.2, -0.9] \cup [0.8, 1.2]$

In **shape+XS+BR** scenario, κ_b limits are comparable with direct searches, while constraints on κ_c improve ($|\kappa_c| < 8.5$ in direct searches)

Effective Field Theory (EFT) interpretation

- ◆ In EFT approach, an effective Lagrangian is defined by \mathcal{L}_{SM} supplemented by additional dimension-6 operators:

$$\mathcal{L}_{EFT} = \mathcal{L}_{SM} + \sum_i \frac{c_i}{\Lambda^2} O_i^{(6)}$$

- ◆ Limits on the Wilson coefficients are obtained using a simultaneous fit to 5 measured cross-sections and their correlations:

$$p_T^{\gamma\gamma}, N_{jets}, m_{jj}, \Delta\phi_{jj} \text{ and } p_T^{j1}$$

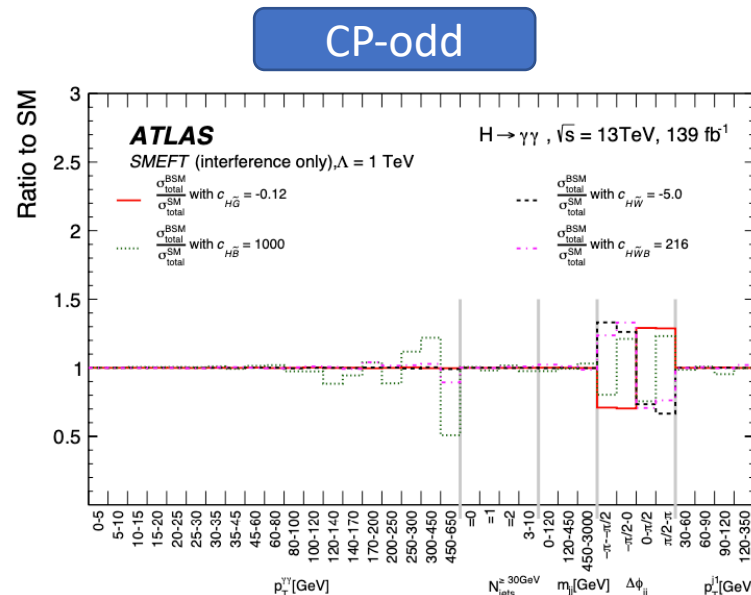
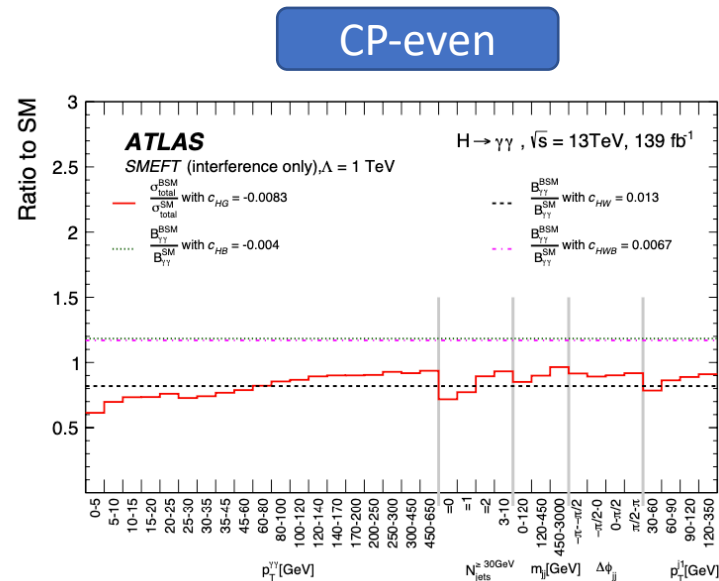
- ◆ In SMEFT formulation, following operators considered. The Wilson coefficients are $c_{HG}, c_{HW}, c_{HB}, c_{HWB}$ and their CP-odd counter-parts

$$\mathcal{L}_{eff}^{SMEFT} \supset c_{HG} O'_g + c_{HW} O'_{HW} + c_{HB} O'_{HB} + c_{HWB} O'_{HWB} + c_{H\bar{G}} \tilde{O}'_g + c_{H\bar{W}} \tilde{O}'_{HW} + c_{H\bar{B}} \tilde{O}'_{HB} + c_{H\bar{W}B} \tilde{O}'_{HWB},$$

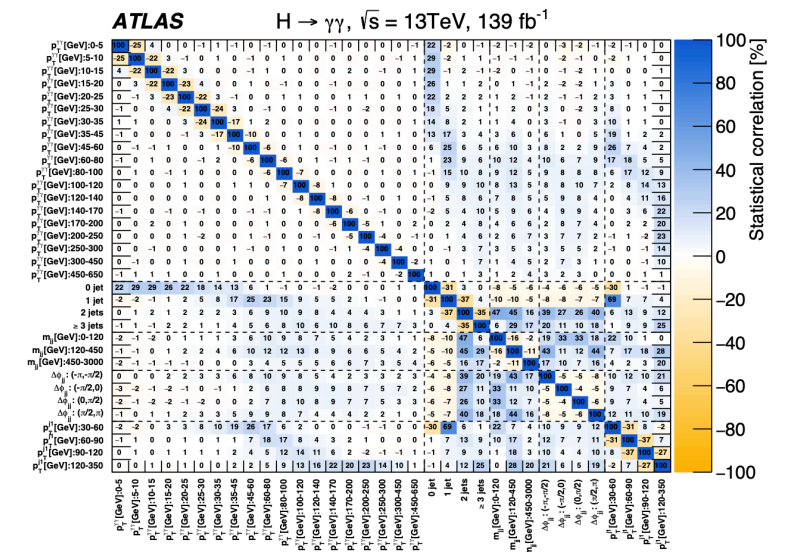
Limits on Wilson coefficients are set by constructing a likelihood function:

$$L = \exp \left[-\frac{1}{2} (\sigma_{obs} - \sigma_{pred})^T C^{-1} (\sigma_{obs} - \sigma_{pred}) \right],$$

Ratio of obs xs to SM as a function of variables: $\left(\frac{d\sigma}{dX}\right)_{c_i} = \sum_j \left(\frac{d\sigma_j}{dX}\right)^{SM} \times \left(\frac{d\sigma_j}{dX}\right)_{c_i}^{MG5} / \left(\frac{d\sigma_j}{dX}\right)_{c_i=0}^{MG5}$



Parameterize σ_{obs} as function of Wilson coefficients



Total statistical correlations among bins of 5 observables

Effective Field Theory (EFT) interpretation

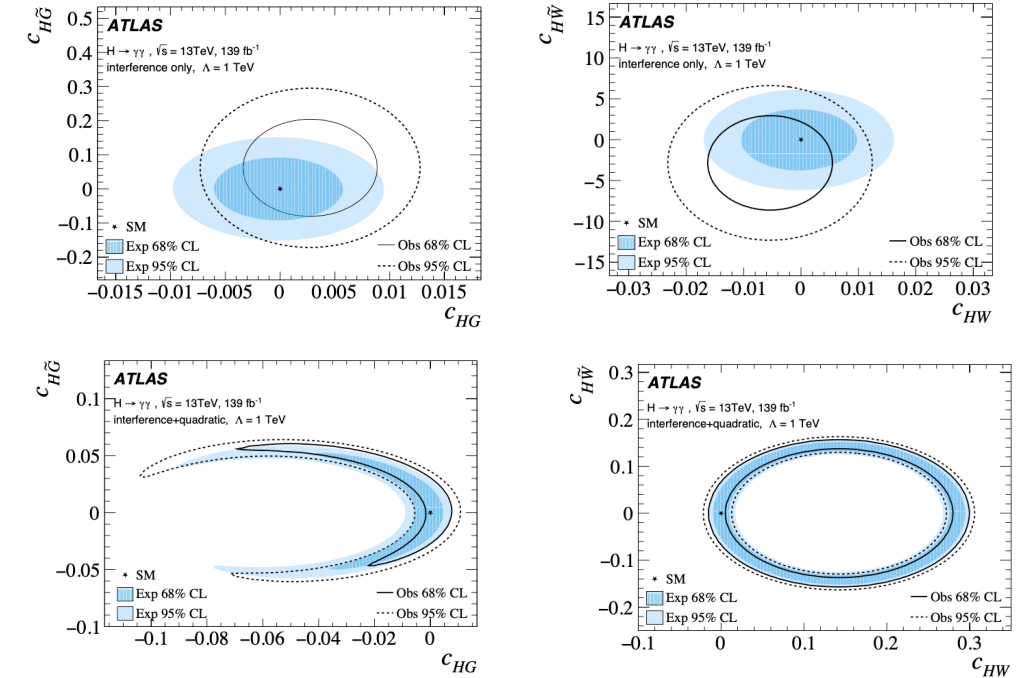
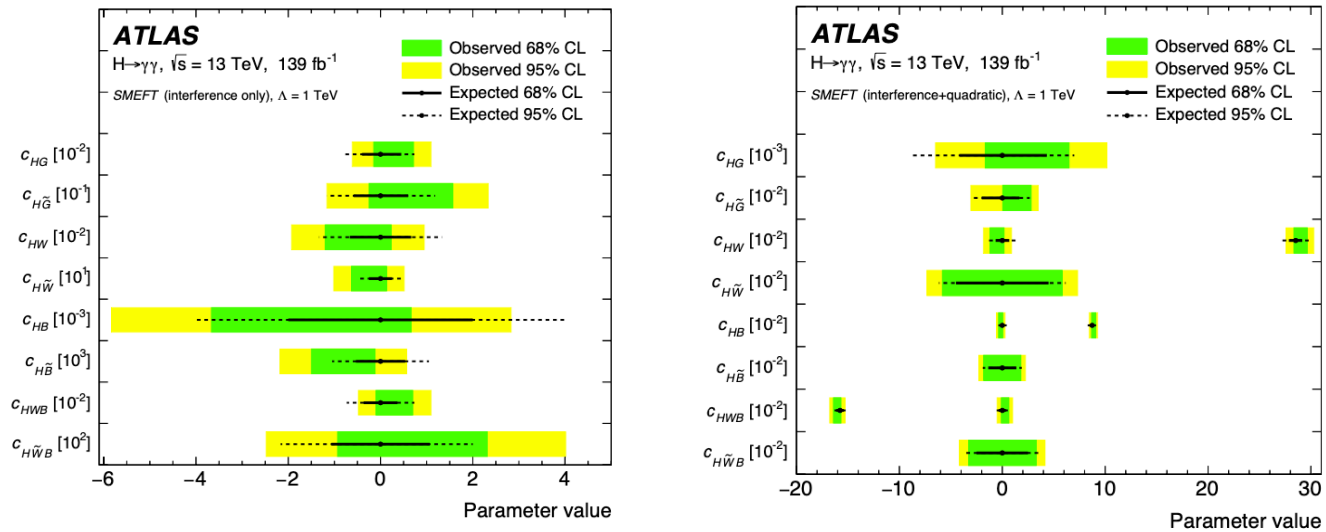
Two scenarios provided. One uses only **interference** terms, and the other uses both **interference** and **quadratic** terms

$$\sigma \times B = \sigma_{\text{SM}} B_{\text{SM}} + \underbrace{(\sigma_{\text{SM}} B_{\text{INT}} + \sigma_{\text{INT}} B_{\text{SM}})}_{\text{Interference terms}} + \underbrace{(\sigma_{\text{SM}} B_{\text{BSM}} + \sigma_{\text{BSM}} B_{\text{SM}})}_{\text{Quadratic terms}} + O(c_i^3/\Lambda^6),$$

Interference terms

Quadratic terms

CP-odd VS CP-even



Coefficient	95% CL, interference-only terms	95% CL, interference and quadratic terms
c_{HG}	$[-6.1, 11.0] \times 10^{-3}$	$[-6.5, 10.2] \times 10^{-3}$
$c_{H\tilde{G}}$	$[-0.12, 0.23]$	$[-3.1, 3.5] \times 10^{-2}$
c_{HW}	$[-1.9, 0.9] \times 10^{-2}$	$[-1.8, 1.0] \times 10^{-2} \cup [0.28, 0.30]$
$c_{H\tilde{W}}$	$[-10.2, 5.2]$	$[-7.3, 7.3] \times 10^{-2}$
c_{HB}	$[-5.8, 2.8] \times 10^{-3}$	$[-5.5, 3.0] \times 10^{-3} \cup [8.4, 9.3] \times 10^{-2}$
$c_{H\tilde{B}}$	$[-21.8, 5.7] \times 10^2$	$[-2.3, 2.3] \times 10^{-2}$
c_{HWB}	$[-5.2, 10.7] \times 10^{-3}$	$[-0.17, -0.15] \cup [-5.5, 9.8] \times 10^{-3}$
$c_{H\tilde{W}B}$	$[-2.5, 4.0] \times 10^2$	$[-4.0, 4.0] \times 10^{-2}$

- ◆ Place stringent limits on all CP-even operators, as they affect primarily normalization of **XS** (c_{HG}) or **BR** (c_{HW} , c_{HB} and c_{HWB})
- ◆ $\Delta\phi_{jj}$ can only constrain $c_{H\tilde{G}}$ and $c_{H\tilde{W}}$ well now. Very loose limits on $c_{H\tilde{B}}$ and $c_{H\tilde{W}B}$ due to lack of sensitivity at current accuracy

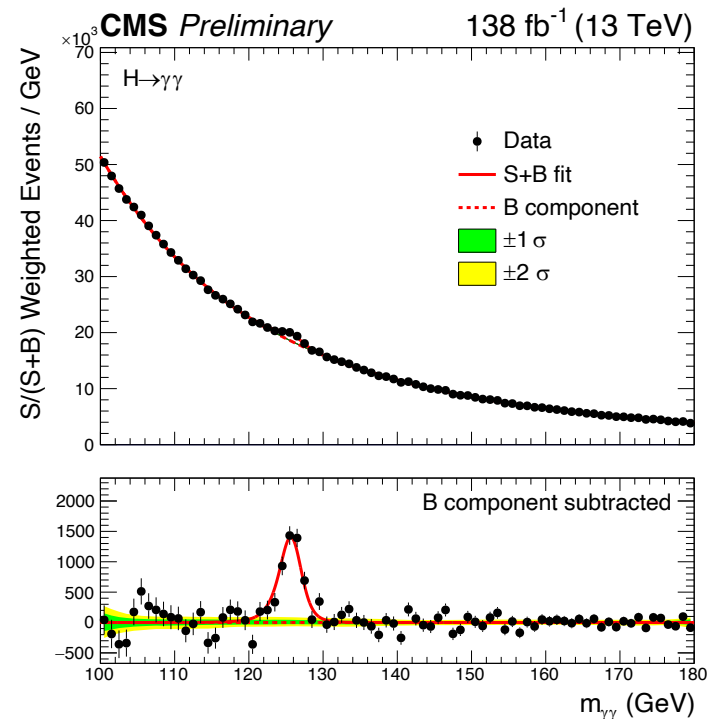
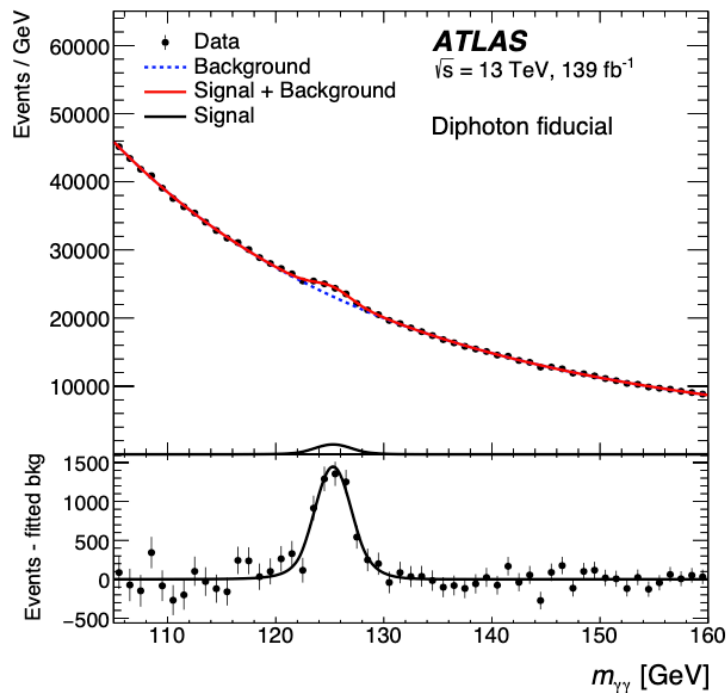
Comparison with CMS paper

Comparison with CMS $H \rightarrow \gamma\gamma$ differential cross-section paper [[link](#)]

Details	ATLAS	CMS
Diphoton fiducial definition	$p_T^{\gamma 1}/m_{\gamma\gamma}(p_T^{\gamma 2}/m_{\gamma\gamma}) > \mathbf{0.35(0.25)}$ $ \eta \in [0,1.37] \cup [1.52,2.37]$	$p_T^{\gamma 1}/m_{\gamma\gamma}(p_T^{\gamma 2}/m_{\gamma\gamma}) > \mathbf{0.33(0.25)}$ $ \eta < 2.5$ Looser criteria
Binning of variables	Not absolutely the same. For example, in high p_T^H region, ATLAS use a finer binning of 250-300-450-650-13000 , while CMS use 250-350-450-∞	
Photon identification	Cut based selection, η/p_T -dependent	BDT-based ID , $\eta/p_T/\rho$ -dependent
Background modeling	From spurious signal study . A dominant systematic uncertainty	From Discrete profiling method . No spurious signal uncertainty introduced
Interpretations	b- and c-quark Yukawa, EFT	Not included

Comparison with CMS paper

	ATLAS	CMS
Measured fiducial cross-sections	<ul style="list-style-type: none"> ◆ SM: 64.2 ± 3.4 fb ◆ <u>Obs</u>: 67 ± 5(stat.) ± 4(sys.) fb rel. stat. error: 7.2% rel. syst error: 6.0% 	<ul style="list-style-type: none"> ◆ SM: 75.44 ± 4.13 fb (due to looser definition) ◆ <u>Obs</u>: $73.40_{-5.3}^{+5.4}$(stat.) $_{-2.2}^{+2.4}$(sys.) fb rel. stat. error: 7.3% rel. syst error: 3.1%



◆ **ATLAS fiducial and differential measurements have similar sensitivity to CMS**, limited by statistical uncertainty. **But systematic uncertainties of CMS are \sim half smaller** (free of spurious signal uncertainty).

◆ An important task for us is to get rid of systematic uncertainty in the next Run3 study!

Conclusion

- ◆ Measurements of Higgs boson fiducial and differential cross-section in diphoton decay channel performed using Full Run2 data collected by ATLAS in 2015-2018. The cross-sections in 5 fiducial phase space volumes and a variety of differential analysis bins get measured and compared with various theoretical predictions. **None of them exhibits significant deviation from predictions**
- ◆ A b- and c-quark Yukawa interpretation and EFT interpretation of some selected observables **place more stringent constraints on BSM models**
- ◆ A comparison with CMS measurements reveals getting rid of systematic uncertainty would be an important task for us in the Run3 period.

Backup

backup

Data and simulation samples

Full Run2 data at $\sqrt{s} = 13$ TeV recorded by ATLAS between 2015-2018 used, with an integrated luminosity of 139.0 fb^{-1} , assuming $m_H = 125.09$ GeV. Events were selected with a trigger requiring $E_T^{\gamma_1}(E_T^{\gamma_2}) > 35(25)$ GeV. Loose identification applied by triggers in 2015-2016 and tightened in 2017-2018

Signal

Powheg+Pythia for all production modes except tH in nominal case. Other generators also used when estimating UEPS/ME uncertainties

Production mode	Generator (ME+PS)	SM predicted $\sigma \times BR$ [fb]	Accuracy of σ
ggF	Powheg NNLOPS+Pythia	110.140	N3LO(QCD), NLO(EW)
VBF	Powheg+Pythia	8.578	approx NNLO(QCD), NLO(EW)
W^+H	Powheg+Pythia	1.902	NNLO(QCD), NLO(EW)
W^-H	Powheg+Pythia	1.206	NNLO(QCD), NLO(EW)
$qq \rightarrow ZH$	Powheg+Pythia	1.725	NNLO(QCD), NLO(EW)
$gg \rightarrow ZH$	Powheg+Pythia	0.279	NLO(QCD), NLO(EW)
$t\bar{t}H$	Powheg+Pythia	1.150	NLO(QCD), NLO(EW)
$b\bar{b}H$	Powheg+Pythia	1.104	NLO(QCD), NLO(EW)
$tHjb$	MG5@NLO+Pythia	0.169	NLO(QCD)
tWH	MG5@NLO+Pythia	0.034	NLO(QCD)
$\gamma\gamma$ +jets, $m_{\gamma\gamma} \in [90,175]$ GeV	Sherpa (ME@NLO+PS)	-	-

background